Theory of the π-periodic motion of two ions in a Paul trap

Marijan Koštrun, Winthrop W. Smith, and Juha Javanainen
Department of Physics, University of Connecticut, Storrs, Connecticut 06269
(Received 19 August 1997)

A theory of the ordered motion of two ions in a Paul trap is derived without using the standard pseudopotential approach. The method relies on the limit cycle theory and the van der Pol–Krylov–Bogoliubov approximation. We evaluate approximate solutions to the equations of motion and discuss stability regions and alignment transition regions for various types of motion. We compare analytical predictions with numerical computations and find a good quantitative agreement. [S1050-2947(98)04204-8]

PACS number(s): 32.80.Pj, 05.45.+b, 47.52.+j

I. INTRODUCTION

A quadrupole Paul trap [1] confines a charged particle dynamically by making use of a static electric (dc) field and a quasistatic radio frequency (ac) field. The device has many applications in single ion spectroscopy and as a possible one ion frequency standard [2]. In most practical applications, however, a Paul trap holds more than one ion, and its operation is affected by the strong Coulomb interactions between the ions. Wuerker, Shelton, and Langmuir demonstrated experimentally [3] that charged microscopic particles confined to a Paul trap show a transition between an ordered ''crystalline'' structure and a disordered cloud. Similar crystals were later observed with laser cooled atomic ions [4,5]. It was proposed in Refs. [6,7] that the melting of the simplest two-ion crystal might be a transition to classical chaos.

While many-ion liquids are well described by straightforward kinetic theory [8], the case of only a few ions calls for a more delicate approach. For two ions the most fruitful one has been the pseudopotential method [9]. The idea is to separate the motion of the ions into two components, fast micromotion and slow secular motion. The secular motion takes place under a pseudopotential obtained by averaging out the micromotion. In Refs. [7,10] it was shown that this approach to some extent reproduces the stability regions in the parameter space of the Paul trap. More recently, an alignment transition was qualitatively predicted [11], i.e., it was shown that by varying the parameters of the trap, the alignment of the ion trajectory changes with respect to the trap axes. The pseudopotential was analyzed in Ref. [10] to see if it allows for chaos in the secular coordinate. Numerically, what is deemed to be secular motion depends strongly on the details of how the micromotion is averaged out, so the question remains unanswered.

In this paper we suggest a novel approach to the two-ion (and potentially few-ion) system. Based on the results of extensive numerical simulations, we conclude that the main characteristic of the orbits of the two ions is the *periodicity*. Accordingly, we analyze in an approximate fashion periodic orbits of two ions, and in particular periodic orbits with the same period as the ac field driving the trap, using the well established technique of limit cycles [12,13].

Under the assumption that the motion is along one of the axes of the trap (radial or along the z axis) the equations of motion can be reduced to a single nonlinear ordinary differential equation to which the limit cycle theory can be applied. In Sec. II we use the van der Pol–Krylov–Bogoliubov approximation to find the limit cycle solutions of the equations of motion. As the result we get trajectories with a rather simple analytical form. We discuss the stability of these trajectories in a manner familiar from the theory of Mathieu-type equations. We demonstrate that for each coordinate (r and z) there exists a region in the parameter space of the trap where a corresponding limit cycle is stable. We refer to those limit cycle solutions as axis aligned motion. In Sec. III we analyze the stability of axis aligned motion by studying the behavior of the coordinate which is supposed not to participate in the limit cycle. We show that there exists a region in which alignment of the trajectory continuously changes, which we call the alignment transition region. We demonstrate that the solutions inside the alignment transition region are a result of mixing of the limit cycles corresponding to the axis aligned motion, and define a mixing parameter θ. Whenever possible, we compare our theoretical results with direct numerical simulations. Section IV gives a discussion and in Sec. V our conclusions are presented.

II. THE AXIS ALIGNED SIMPLE HARMONIC MOTION

In classical terms, the motion of two identical ions in a Paul radio frequency trap can be described with two sets of differential equations. The first set describes the motion of the center of mass of the system. It consists of three Mathieu-type equations, one for the axial (z) motion and two equations of the same form for the transverse coordinates (x and y). The Paul trap is taken into account in these equations via two dimensionless parameters. In the literature [14,7] they are often referred to as (a,q). These correspond to the dc and ac amplitudes of the trap field, respectively. Effects of the laser or other cooling on the motion of the ions are taken into account via a damping parameter γ. Using this notation, a Mathieu equation for the motion of the center of mass can be written as

$$\ddot{x}^{(K)} = -\gamma \dot{x}^{(K)} - K[a + 2q\ \cos(2\tau)]x^{(K)}. \tag{1}$$

The index $K = 1, -2$ pertains to the equation for the r, z coordinate, respectively. The nature of the solutions to the Mathieu equation is well known and documented in the literature [15,13,16,12]. For the purposes of this paper, the

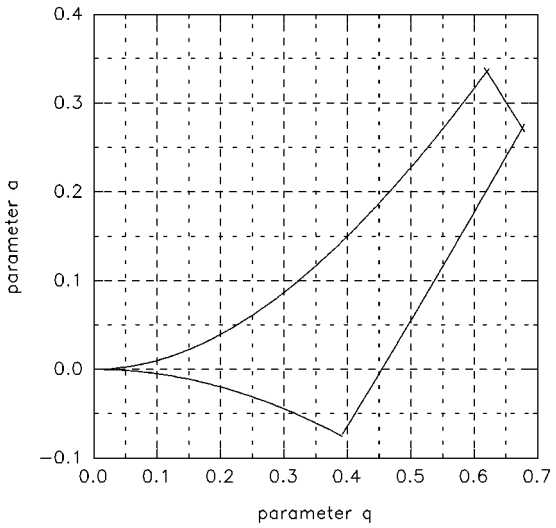

FIG. 1. Mathieu single-ion stability region (MSISR) in the (a,q) parameter space. The boundaries are calculated numerically by using Floquet's theorem. For any choice of dimensionless parameters (a,q) within the MSISR the motion of the center of mass of two ions is stable.

most interesting aspect is the stability region in the (a,q) parameter space. It represents the set of parameters (a,q) of the trap for which the center of mass performs damped periodic motion. Each coordinate has its own stability region. The intersection of these regions is referred to as the Mathieu single-ion stability region (MSISR) [7] and is depicted in Fig. 1. An analytical approximation to the boundaries of MSISR in the small γ limit ($\gamma \ll 1$) is given by

$$-\frac{1}{2}q^2 \leqslant a \leqslant 1-q, \qquad -\frac{1}{2}+q \leqslant a \leqslant q^2. \tag{2}$$

Details may be found in Refs. [17,16,13,15].

A second set describes the relative motion of the two ions. Using the cylindrical symmetry of the trap, the following system of differential equations is obtained:

$$\frac{d^2r}{d\tau^2} = -\gamma\frac{dr}{d\tau} - [a+2q\,\cos(2\tau)]r + \frac{r}{(r^2+z^2)^{3/2}}, \tag{3}$$

$$\frac{d^2z}{d\tau^2} = -\gamma\frac{dz}{d\tau} + 2[a+2q\,\cos(2\tau)]z + \frac{z}{(r^2+z^2)^{3/2}}.$$

These equations have been made dimensionless by distance and time scaling.[1] A detailed derivation along with the scaling procedure can be found in Ref. [14]. In this paper, the axis aligned motion will be understood to mean the solutions to Eq. (3) obtained when one of the coordinates is zero. The system (3) then reduces to

$$\frac{d^2x^{(K)}}{d\tau^2} = -\gamma\frac{dx^{(K)}}{d\tau} - K[a+2q\,\cos(2\tau)]x^{(K)} + \frac{\mathrm{sgn}(x^{(K)})}{(x^{(K)})^2}, \tag{4}$$

where the function $\mathrm{sgn}(x)$ is $+1$ if $x>0$ and -1 if $x<0$. The choice $K=1$ or $K=-2$ yields equations for the r or the z coordinate, respectively. Due to the singularity of the Coulomb interaction at $x^{(K)}=0$, $x^{(K)}$ cannot change sign. Without loss of generality, we may thus assume that $x^{(K)}(\tau)>0$ at all times.

We now proceed to calculate limit cycles of Eq. (4) using the van der Pol–Krylov–Bogoliubov approximation. We estimate the stability regions of these solutions within the boundaries of the MSISR and develop analytical approximations to the boundaries of different regions. We compare the analytical expressions for the boundaries to the ones obtained numerically.

A. π-periodic limit cycle

We begin by examining the limit cycle solution to Eq. (4) that has the period of π, the same as the period of the ac field of the trap. We start, in the spirit of the van der Pol–Krylov–Bogoliubov approximation, from the ansatz that the asymptotic solution to Eq. (4) in phase space approximates a closed circular orbit. We express this orbit by the form

$$x^{(K)} = x_0^{(K)} + \delta x^{(K)}\,\cos(2\tau+\phi^{(K)}), \tag{5}$$

$$\dot{x}^{(K)} = -2\,\delta x^{(K)}\sin(2\tau+\phi^{(K)}), \tag{6}$$

where $x_0^{(K)}$ is a positive constant yet to be determined, the result of opposite actions of friction (that tends to shrink the orbit to the origin) and Coulomb repulsion (that has singularity at the origin). The amplitude $\delta x^{(K)}$, which is positive by choice, and the phase $\phi^{(K)}$, which is constrained to the interval $[0,2\pi]$, are allowed to vary slowly over a time scale much longer than the period π. Calculating the time derivative from Eq. (5) and comparing to Eq. (6) we obtain a constraint, our first equation

$$\delta\dot{x}^{(K)}\,\cos(2\tau+\phi^{(K)}) - \delta x^{(K)}\dot{\phi}^{(K)}\,\sin(2\tau+\phi^{(K)}) = 0. \tag{7}$$

The second equation is obtained by taking the derivative of Eq. (6):

$$\ddot{x}^{(K)} = -4\,\delta x^{(K)}\cos(2\tau+\phi^{(K)}) - 2\,\delta\dot{x}^{(K)}\sin(2\tau+\phi^{(K)}) - 2\,\delta x^{(K)}\dot{\phi}^{(K)}\cos(2\tau+\phi^{(K)}). \tag{8}$$

We now insert Eq. (8) into Eq. (4) and expand the Coulomb term as a power series in $\delta x^{(K)}/x_0^{(K)}$ to second order using Eq. (5). The resulting equation, together with Eq. (7), constitutes a system for $\delta\dot{x}$ and $\delta x\dot{\phi}$. Averaging this system with the weights 1, $\cos(2\tau+\phi)$, and $\sin(2\tau+\phi)$, respectively, over the period π gives

[1]The scaling distance used in the present paper is $d^3=8e^2/4\pi\epsilon_0 m\omega^2$. It is independent of the parameters a and q. This differs from the scaling of the distance used in Refs. [14,7,10], which includes both a and q. The time is in units of $2/\omega$. Frequency ω corresponds to the ac driving field of the trap.

$$\delta\dot{x}^{(K)} = -\frac{1}{2}\gamma\delta x^{(K)} + \frac{1}{2}Kqx_0^{(K)}\sin(\phi^{(K)}), \tag{9}$$

$$\delta x^{(K)}\dot{\phi}^{(K)} = \left(-1 + \frac{Ka}{4} + \frac{1}{2(x_0^{(K)})^3}\right)\delta x^{(K)} + \frac{1}{2}Kqx_0\cos(\phi^{(K)}), \tag{10}$$

$$0 = -Kax_0^{(K)} + \frac{1}{(x_0^{(K)})^2} - Kq\,\delta x^{(K)}\cos(\phi^{(K)}). \tag{11}$$

The limit cycle is a solution to the system (9)–(11) with the time derivatives on the left hand sides equated to zero. The system of equations then becomes

$$-\frac{1}{2}\gamma\delta x^{(K)} + \frac{1}{2}Kqx_0^{(K)}\sin(\phi^{(K)}) = 0, \tag{12}$$

$$\left(-1 + \frac{Ka}{4} + \frac{1}{2(x_0^{(K)})^3}\right)\delta x^{(K)} + \frac{1}{2}Kqx_0^{(K)}\cos(\phi^{(K)}) = 0, \tag{13}$$

$$-Kax_0^{(K)} + \frac{1}{(x_0^{(K)})^2} - Kq\,\delta x^{(K)}\cos(\phi^{(K)}) = 0. \tag{14}$$

If we assume that $\delta x^{(K)} > 0$, $x_0^{(K)} > 0$, and $\delta x^{(K)}/x_0^{(K)} \ll 1$, and that γ and q are small positive numbers of the order $\delta x^{(K)}/x_0^{(K)}$ or smaller, then Eq. (12) yields $|\sin(\phi^{(K)})| \ll 1$. Since the two K's are of opposite sign, for $K=1$ we obtain $0 < \sin(\phi) \ll 1$, or $\sin(\phi) \approx \phi$. For $K=2$ analogously $0 < -\sin(\phi) \ll 1$, or $\phi = \pi + \varphi$. This allows us to replace the trigonometric functions of $\phi^{(K)}$ in Eqs. (12)–(14) with

$$\sin(\phi^{(K)}) \approx \mathrm{sgn}(K)\,\phi^{(K)}, \qquad \cos(\phi^{(K)}) \approx \mathrm{sgn}(K). \tag{15}$$

After this simplification, Eqs. (12)–(14) can be solved. The solutions for the limit cycle of the r coordinate are

$$r_0^3 = \frac{8 - 2a - 2q^2 - \frac{3}{2}aq^2}{2(4a - a^2 + q^2)}, \tag{16}$$

$$\frac{\delta r}{r_0} = -\frac{a}{q} + \frac{1}{qr_0^3} = \frac{(4 + 4a + 3a^2)q}{16 - 4a - 4q^2 - 3aq^2}, \tag{17}$$

$$\phi = \frac{\gamma}{q}\frac{\delta r}{r_0}. \tag{18}$$

The respective solutions for the limit cycle of the z coordinate are

$$z_0^3 = \frac{4 + 2a - 4q^2 + 6aq^2}{2(-4a - 2a^2 + 4q^2)}, \tag{19}$$

TABLE I. Comparison of the theoretical results $(r_{\mathrm{theor}}, \delta r_{\mathrm{theor}})$ for the limit cycles, Eqs. (16), (17) with the results $(r_{\mathrm{expt}}, \delta r_{\mathrm{expt}})$ of numerical computations. For each set of parameters the relative error of the analytical approximation with respect to the numerical value is also given.

a	q	r_{theor}	r_{expt}	Rel. error (%)	$\delta r_{\mathrm{theor}}$	δr_{expt}	Rel. error (%)
0	0.05	9.3	9.4	1	0.23	0.23	1
0	0.1	5.8	5.9	1	0.29	0.29	1
0.01	0.15	3.6	3.7	3	0.27	0.27	1
0.015	0.2	3	3.1	2	0.31	0.31	1
0.02	0.25	2.7	2.7	1	0.34	0.35	1
0.03	0.3	2.3	2.4	2	0.37	0.37	1
0.04	0.35	2.1	2.2	4	0.39	0.4	1
0.056	0.4	1.9	2	4	0.42	0.43	2

$$\frac{\delta z}{z_0} = \frac{a}{q} + \frac{1}{2qz_0^3} = \frac{(2 - 2a + 3a^2)q}{2 + a - 2q^2 + 3aq^2}, \tag{20}$$

$$\varphi = \frac{\gamma}{2q}\frac{\delta z}{z_0}. \tag{21}$$

We require that the solutions (16) and (19) are positive. This yields, keeping in mind that (a,q) is inside MSISR and γ is less than 1, the conditions

$$4a - a^2 + 2q^2 > 0, \qquad -2a - a^2 + 2q^2 > 0. \tag{22}$$

These conditions are to be compared with the boundaries of the MSISR [15], Eq. (2), that we started with. We see that close to the origin the stability boundaries of the axis aligned motion of two ions in a Paul trap, solutions of Eq. (4), are the same up to the order of a^2 as the boundaries of the MSISR, Eq. (2). This similarity is due to the nature of the Coulomb interaction. As can be seen from Eqs. (16) and (19), close to the boundary $r_0 \to \infty$ (or $z_0 \to \infty$), hence the contribution of the Coulomb term of Eq. (4) is rather small so that Eq. (4) is reduced to the Mathieu equation (1).

We have compared the results thus obtained to numerical simulations. For the latter, the fourth order Runge-Kutta method was used. The time step of $\pi/100$ proved to be small enough to satisfy the precision requirements. The value of the parameter γ was fixed at 0.01. Before taking data, the system was allowed to settle for 1000 − 10 000 periods of the driving field. The computations were performed using initial conditions $(r,\dot{r},z,\dot{z})_0 = (1,0,0,0.1)$. We then calculated the autocorrelation function [18] and performed other checks to assure that the period of the solution was π. The parameters (a,q) were chosen so that the axis aligned motion of a particular coordinate was obtained as well. For each π-periodic and axis aligned orbit, average and peak-to-peak amplitude variation were calculated over one period of the driving field. The average was identified as r_0, z_0 and the oscillation amplitude as twice $\delta r, \delta z$, respectively. The results are shown in Tables I and II. An example of a π-periodic orbit obtained

TABLE II. Comparison of the theoretical results $(z_{\text{theor}}, \delta z_{\text{theor}})$ for the limit cycles, Eqs. (19) and (20), with the results $(z_{\text{expt}}, \delta z_{\text{expt}})$ of numerical computations. For each set of parameters the relative error of the analytical approximation with respect to the numerical value is also given.

a	q	z_{theor}	z_{expt}	Rel. error (%)	δz_{theor}	δz_{expt}	Rel. error (%)
0.008	0.1	6.3	6.4	1	0.63	0.63	1
0.035	0.2	4.8	4.9	2	0.95	0.97	2
0.07	0.3	3	3.1	3	0.89	0.92	4
0.12	0.4	2.6	2.7	5	0.99	1.07	7
0.15	0.45	2.2	2.4	7	0.97	1.07	10
0.2	0.5	2.5	2.7	9	1.15	1.3	11
0.25	0.55	2.8	2.9	5	1.37	1.49	8
0.3	0.6	3.1	3.2	4	1.63	1.72	5

numerically, together with a limit cycle defined by Eqs. (19), (20), is given in Fig. 2.

We conclude that our analytical approximations for the limit cycles generally agree to within a few percent with the numerical solutions to Eq. (4), and accordingly the axis aligned motion of Eq. (3) is also adequately approximated. This is valid in the regions of the MSISR where π-periodic orbits may exist.

B. Stability of the π-periodic limit cycle of Eq. (4)

We analyze stability of the limit cycles for each of the coordinates using the methods derived for Mathieu-type differential equations, described in Refs. [12,15,13,16,19]. We start by stating the basic properties of the solutions to the Mathieu equation (1). We then show how these properties

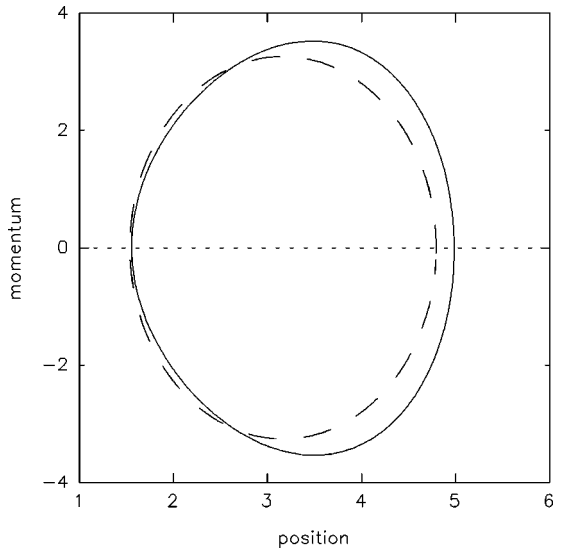

FIG. 2. Numerical solution (solid line) with the period π to the system (3) is shown here in phase space, along with a limit cycle (dashed line) that follows from the van der Pol–Krylov–Bogoliubov approach, Eqs. (16)–(18) and (19)–(21). In this particular case the choice of the parameters was $\gamma=0.01$, $(a,q)=(0.3, 0.6)$, and the initial conditions were $(r,\dot{r},z,\dot{z})=(1,0,0,0.1)$. All times, distances, and velocities are rendered dimensionless with a scaling discussed in the text.

can be used to obtain the stability boundaries of Eq. (4), provided the nonlinear term in Eq. (4) is linearized using our analytical approximation for the limit cycles. In the end, we give comparisons with numerical results.

The Mathieu differential equation (1) is a second order linear differential equation with periodic coefficients. It is convenient to write the solutions as Fourier sums. Owing to the $\cos(2\tau)$ coupling in Eq. (1), two linearly independent solutions may be chosen in such a way that one only contains even frequencies $(0,2,4,\ldots)$ and the other only odd frequencies $(1,3,5,\ldots)$. At a boundary of the stability region, one of these becomes unstable. A boundary in the (a,q) parameter space thus represents the set of values for which the Mathieu equation (1) has one bounded solution with the period π or 2π, and the other solution is about to turn unbounded.

The nonlinear Coulomb repulsion in Eq. (4) causes mixing of the odd and even frequency solutions. However, to the lowest order in the parameters a and q, the solutions to Eq. (4) display the same decoupling of even and odd time evolution as the Mathieu equation. This allows us to extract information about the boundaries by observing separately the behavior of the limit cycles with periods π and 2π. Solutions to Eq. (4) with the periods π and 2π do not have the same importance. A solution with the period π is self-sustaining and has an asymptotic nonzero behavior in the form of a limit cycle, as shown earlier. A solution with the period 2π has a different property. As will be shown by analyzing its limit cycle, a 2π-periodic limit cycle can be sustained only by perturbation, i.e., in the stable region of Eq. (4) this component dies out exponentially due to the damping. However, if by the choice of the parameters (a,q) the 2π-periodic component becomes unstable, even if the π-periodic solution is in the stable region, the system will be unstable.

Following [13], we examine how the system behaves if the limit cycle with a period of 2π is imposed as a solution to Eq. (4). Using the van der Pol–Krylov–Bogoliubov approximation, we chose instead of Eqs. (5) and (6) the following form for the limit cycle:

$$y^{(K)}=y_0^{(K)}+\delta y^{(K)}\cos(\tau+\vartheta^{(K)}), \tag{23}$$

$$\dot{y}^{(K)}=-\delta y^{(K)}\cos(\tau+\vartheta^{(K)}). \tag{24}$$

We then proceed, in analogy with Eqs. (12)–(14), to obtain

$$\delta\dot{y}^{(K)}=\frac{1}{2}qK\delta y^{(K)}\sin(2\vartheta^{(K)}), \tag{25}$$

$$\dot{\vartheta}^{(K)}=-\frac{1}{2}+\frac{1}{2}Ka+\frac{1}{2}Kq\cos(2\vartheta^{(K)})+\frac{1}{(y_0^{(K)})^3}, \tag{26}$$

$$0=Kay_0^{(K)}-\frac{1}{(y_0^{(K)})^3}. \tag{27}$$

In Eq. (25) we have confirmed that the amplitude of 2π-periodic component $\delta y^{(K)}$ is independent of $y_0^{(K)}$ (in the limit when $a\to 0$, $y_0^{(K)}\to x_0^{(K)}$). From Eq. (25), the general behavior of the 2π-periodic limit cycle can be inferred, as

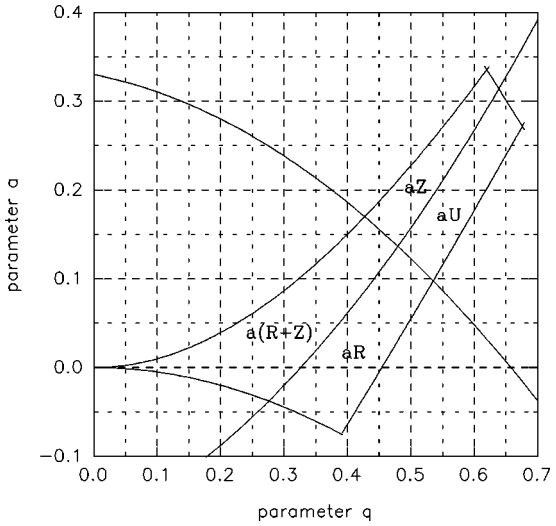

FIG. 3. Stability regions of the limit cycle solutions of Eq. (4), for the r and z coordinates. The boundaries of different regions are obtained theoretically and numerically in Sec. II. Here only the numerical values given by Eqs. (30) and (31) are shown. In the aR (aZ) region a π-periodic motion for r coordinate (z) is stable. In the $a(R+Z)$ a π-periodic limit cycle motion of both coordinates is stable, while in the aU region the limit cycle of neither coordinate is stable.

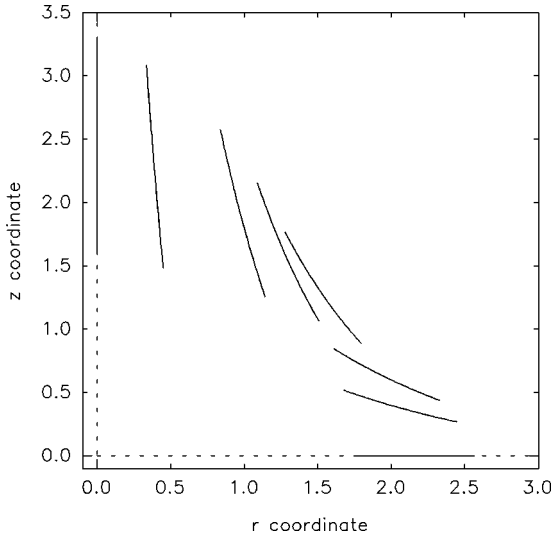

FIG. 4. Behavior of the π-periodic orbits in (r,z) space when the parameters (a,q) are inside the transition region. The values of the parameters are $\gamma=0.01$, $q=0.35$, and $a=0.048$ (r alignment), 0.055, 0.060, 0.065, 0.070, 0.075, and 0.080 (z alignment).

indicated earlier. If 2π-periodic motion is in the stable region, then δy decays exponentially and the 2π-periodic limit cycle eventually becomes unimportant. In the contrary case δy grows exponentially, thus destroying the presumed form of the solution (7) for π-periodic orbits just as well.

We find that for $K=1$, the fixed point is at $\vartheta=\pi/4$, and for $a\leqslant\frac{1}{3}-\frac{1}{3}q$, system (4) is stable under small perturbations. Similarly, for $K=-2$, the fixed point is at $\vartheta=-\pi/4$, and for $a\geqslant-\frac{1}{6}+\frac{1}{3}q$, the system is again stable under small perturbations. The analytical approximation of the stability boundaries of Eq. (4) is given by

$$-\frac{q^2}{2}\leqslant a\leqslant\frac{1}{3}-\frac{q}{3}, \tag{28}$$

$$-\frac{1}{6}+\frac{q}{3}\leqslant a\leqslant q^2. \tag{29}$$

The condition (28) is for $K=1$(r coordinate) and Eq. (29) for $K=-2$ (z coordinate). Other methods can be employed for the studies of these boundaries [20,21]. To the lowest order in q they all yield the same result, but require more tedious calculations.

We have also performed a numerical analysis of the stability boundaries of Eq. (4) for each coordinate. In the computations we used the initial condition $(x,\dot{x})_0=(x_0,0)$, where x_0 was calculated from Eqs. (16) and (19). We found that the stability regions can be closely approximated by

$$-0.5q^2\leqslant a\leqslant 0.33-0.14q-0.55q^2, \tag{30}$$

$$-0.18+0.32q+0.71q^2\leqslant a\leqslant q^2, \tag{31}$$

for the r and z coordinate, respectively. Figure 3 shows the stability regions of Eq. (4) inside MSISR. We see four regions. In regions aR (aZ) a limit cycle of the r (z) coordinate is stable. In region $a(R+Z)$ both r and z coordinate limit cycles are stable, and in the region aU Eq. (4) does not have a stable π-periodic limit cycle.

A comparison between Eq. (28) and Eq. (30) shows that for the r coordinate we have reached only a fair degree of agreement between the numerical and approximate analytical results. For the z coordinate, the agreement is better. The analytical results are, of course, limited in that the analysis is based on linearization of the Coulomb repulsion around a limit cycle orbit.

III. OFF-AXIS SIMPLE HARMONIC MOTION

It was observed in numerical simulations that the system (3) supports off-axis π-periodic orbits for certain choices of the parameters (a,q) inside the MSISR. We call the part of the (a,q) parameter space that supports such orbits the ''transition region.'' The spatial shape of the off-axis π-periodic orbits is illustrated in Fig. 4, where the parameter values were $\gamma=0.01$, $q=0.35$, and $a=0.04$ (r axis alignment), 0.048, 0.050, 0.055, 0.060, 0.065, 0.070, and 0.080 (z axis alignment). Figure 5 shows that the behavior of the alignment of the π-periodic orbits is parameter dependent. We plot the averages of the r and z coordinates, calculated in the same manner that was used for the numerical assessment of the limit cycles. The parameter q was held fixed at the value of 0.3, we chose $\gamma=0.01$, and the parameter a was changed in the interval [0.037, 0.048]. From these computed results it follows that a π-periodic orbit in the transition region is still one dimensional but off axis. The results of Sec. II, which were derived for the axis aligned motion, cannot be directly used.

We suggest two approaches to analyze the behavior of the system (3) inside the transition region: the Mathieu equation approach, and the action functional approach. Together with

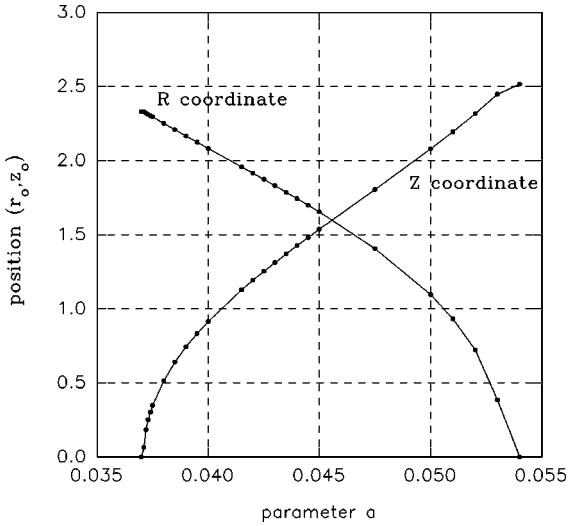

FIG. 5. Behavior of the π-periodic solution to the system (3) inside the transition region. The position represents particular coordinate averaged over one period. With $\gamma=0.01$ and $q=0.3$ constant, a smooth transition of alignment with respect to the parameter a can be seen.

the results of Sec. II they allow us to evaluate the boundaries of the transition region and study the nature of the simple harmonic (π-periodic) orbits that occur within that region. We compare the results of these two theoretical approaches with numerical simulations.

A. Mathieu equation approach

Figure 5 demonstrates a very important property of the π-periodic orbits close to the boundary between the axis aligned and transition region: one of the coordinates is still in its limit cycle, while the other starts to emerge slowly with the change of one of the parameters. This is the basis for our analysis of the transition boundary, as it allows the application of the results from the theory of Mathieu-type differential equations.

We assume that one of the coordinates is in its limit cycle. Therefore it is described by the limit cycle equations, Eqs. (16)–(18) or Eqs. (19)–(21). The other (suppressed) coordinate will perform the motion that will be described by a modified Mathieu equation that follows when the contribution of the *suppressed* coordinate is neglected in the Coulomb repulsion term. The axis aligned motion will be stable as long as the modified Mathieu equation[2] that describes the suppressed coordinate is in the stable region.

For simplicity, let us suppose that the r coordinate is suppressed and the z coordinate is the limit cycle coordinate, the parameters of the limit cycle being given in Eqs. (19)–(21). The equation that governs the behavior of r can be closely approximated by

$$\ddot{r}=-\gamma\dot{r}-[a+2q\,\cos(2\tau)]r+\frac{r}{z^3}. \tag{32}$$

[2]We use the property of the solution of the Mathieu equation with nonzero friction that in the stable region the solution is damped. See, for example, Ref. [4].

We expand the $1/z^3$ term in powers of $\delta z/z_0$, keeping track of the phase shift of the z coordinate up to the second order. Using the trigonometric relationship $\cos^2(2\tau)=1/2+(1/2)\cos(4\tau)$ and neglecting the second harmonic term $\cos(4\tau)$, we obtain

$$\frac{1}{z^3}\simeq\frac{1}{z_0^3}+3\frac{\delta z^2}{z_0^5}+3\frac{\delta z}{z_0^4}\cos(2\,\tau). \tag{33}$$

This allows us to deduce how the limit cycle of the z coordinate modifies the parameters (a,q) to (a^*,q^*) in the corresponding Mathieu equation (1) for the r coordinate. We get after simple manipulations

$$\begin{aligned} a^*&=a-\frac{1}{z_0^3}-3\frac{\delta z^2}{z_0^5},\\ q^*&=q-\frac{3}{2}\frac{\delta z}{z_0^4}. \end{aligned} \tag{34}$$

Using the values of the z coordinate limit cycle from Eqs. (19)–(21) and the condition (22) for the r coordinate with these modified parameters, we obtain the following condition of stability:

$$a\geqslant\frac{1}{2}q^2+\frac{5}{3}q^4. \tag{35}$$

We conclude that if the conditions (35) and (31) are satisfied, the system (3) will oscillate in the z direction and will be stable against perturbations in the r direction. For the other coordinate, the stability condition becomes

$$a\leqslant\frac{1}{2}q^2-\frac{41}{48}q^4. \tag{36}$$

One is again led to conclude that if Eqs. (36) and (30) are satisfied, the system (3) may oscillate along the r axis, for it is stable against perturbations in the z direction.

Even though our analytical arguments so far do not account for the alignment transition region, they nonetheless turn out to give a good qualitative picture about the stability regions of the axis aligned motion. We now proceed to an analytical treatment of the alignment transition itself.

B. Action functional in the limit cycle approximation

We examine theoretically the nature of the π-periodic solutions inside the transition region. Figures 5 and 6 suggest two approaches.

By the first one, one performs a rotation of the (r,z) coordinate system by some angle θ in the hope that in the new coordinates the system (3) may have a simple form to which the results of Sec. II can be applied. Unfortunately, that will not work. In any new coordinates the system (3) has a close to intractable form, and even in the lowest order of approximation, it seems that nothing can be inferred about the angle θ.

The second approach is based on the assumption that the off-axis π-periodic orbit can be represented as a mixture of

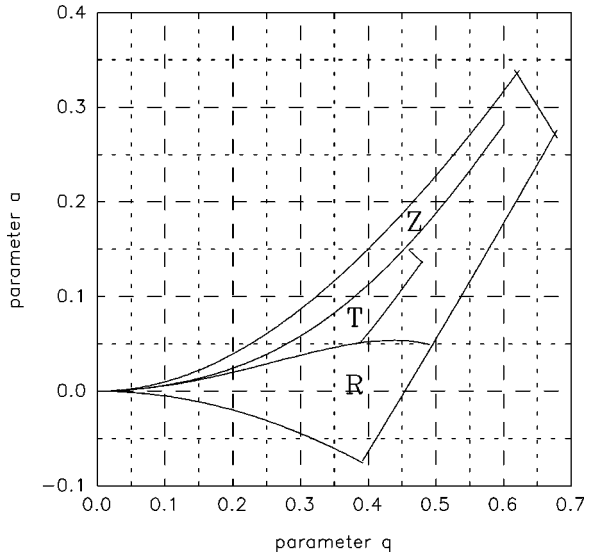

FIG. 6. The MSISR is shown together with the three alignment regions of Eq. (3). For boundaries, the numerically obtained values from Eqs. (42) and (43) are given. In the $R(Z)$ region a π-periodic limit cycle of the $r(z)$ axis aligned motion is stable. In the T region the π-periodic limit cycles are not axis aligned and/or the periodic orbits with multi-π period may occur.

the limit cycles of the axis aligned motion. We introduce a mixing parameter θ and calculate the action functional for the system (3). Alignment of the system is obtained as the value of the angle θ at which the action functional has an extremum.

Following the latter approach, we introduce the mixing angle θ in the following fashion. We assume that the r and z coordinates of the off-axis orbit can be written as

$$\begin{aligned} r &= \cos(\theta) r_{\rm lim} = \cos(\theta)[r_0 + \delta r\ \cos(2\tau)], \\ \dot{r} &= -\cos(\theta)\dot{r}_{\rm lim} = -\cos(\theta) 2\,\delta r\ \sin(2\tau), \end{aligned} \tag{37}$$

$$\begin{aligned} z &= \sin(\theta) z_{\rm lim} = \sin(\theta)[z_0 - \delta z\ \cos(2\tau)], \\ \dot{z} &= \sin(\theta)\dot{z}_{\rm lim} = \sin(\theta) 2\,\delta z\ \sin(2\tau). \end{aligned} \tag{38}$$

We have $r_0, \delta r$ from Eqs. (16) and (17), and $z_0, \delta z$ from Eqs. (19) and (20) as functions of the parameters (a,q). The angle $\theta = 0$ corresponds to the axis aligned motion of the r coordinate, while the angle $\theta = \pi/2$ corresponds to the axis aligned motion of the z coordinate.

The Lagrangian $\mathcal{L}$ of the system (3) can be written

$$\begin{aligned} \mathcal{L}(a,q,\theta,\tau) = &\frac{1}{2}[\cos^2(\theta)\dot{r}_{\rm lim}^2 + \sin^2(\theta)\dot{z}_{\rm lim}^2] \\ &- \frac{1}{2}[a + 2q\ \cos(2\tau)] \\ &\times [\cos^2(\theta) r_{\rm lim}^2 - 2\sin^2(\theta) z_{\rm lim}^2] \\ &- \frac{1}{[\cos^2(\theta) r_{\rm lim}^2 + \sin^2(\theta) z_{\rm lim}^2]^{1/2}}. \end{aligned} \tag{39}$$

The action $\mathcal{S}$ of the corresponding Lagrangian $\mathcal{L}$ is given by

$$\mathcal{S}(a,q,\theta) = \int_0^\pi d\tau \mathcal{L}(a,q,\theta,\tau). \tag{40}$$

We find the extrema of the action $\mathcal{S}$ with respect to the mixing angle θ. Partial differentiation with respect to θ gives

$$\begin{aligned} \frac{\partial \mathcal{S}}{\partial \theta} = &\sin(\theta)\cos(\theta) \\ &\times \int_0^\pi d\tau \Bigg(-\dot{r}_{\rm lim}^2 + \dot{z}_{\rm lim}^2 + [a + 2q\ \cos(2\tau)](r_{\rm lim}^2 + 2z^2) \\ &- \frac{r_{\rm lim}^2 - z_{\rm lim}^2}{[\cos^2(\theta) r_{\rm lim}^2 + \sin^2(\theta) z_{\rm lim}^2]^{3/2}} \Bigg). \end{aligned} \tag{41}$$

By solving Eq. (41) for $\partial\mathcal{S}/\partial\theta = 0$ we obtain three solutions. Two of them are trivial, 0 and $\pi/2$. A third solution θ_3, inside the transition region, is in the interval $[0, \pi/2]$. When the boundary of a stability region is approached, the angle θ_3 approaches either 0 or $\pi/2$. We conclude that on the boundary $\theta = 0$ or $\theta = \pi/2$ is a double root of Eq. (41). This yields

$$\begin{aligned} \int_0^\pi d\tau \Bigg[&-\dot{r}_{\rm lim}^2 + \dot{z}_{\rm lim}^2 + [a + 2q\ \cos(2\tau)](r_{\rm lim}^2 + 2z_{\rm lim}^2) \\ &- \frac{1}{r_{\rm lim}} + \frac{z_{\rm lim}^2}{r_{\rm lim}^3} \Bigg] = 0, \end{aligned} \tag{42}$$

$$\begin{aligned} \int_0^\pi d\tau \Bigg[&-\dot{r}_{\rm lim}^2 + \dot{z}_{\rm lim}^2 + [a + 2q\ \cos(2\tau)](r_{\rm lim}^2 + 2z_{\rm lim}^2) \\ &- \frac{r_{\rm lim}^2}{z_{\rm lim}^3} + \frac{1}{z_{\rm lim}} \Bigg] = 0. \end{aligned} \tag{43}$$

Equation (42) is satisfied at the boundary between the r axis alignment region and transition region, and similarly Eq. (43) will be satisfied at the boundary between the z axis aligned region and the transition region. Within the limit cycle approximation these integrals can be calculated exactly using contour integral techniques (see the Appendix). We have used them to obtain the boundary numerically, but independently of direct numerical computations.

C. Direct numerical computations

We have computed the boundaries of the transition region numerically in a manner similar to that underlying Fig. 5. We choose a few values of the parameter q for which we obtain π-periodic orbits. For each value of the parameter q the corresponding value of the parameter a is located inside the transition region, but close to the boundary. The critical value of the parameter a is chosen so that the amplitude of the suppressed coordinate is small but does not decrease with the increase of the number of thermalization steps (number of periods during which the system was allowed to settle down). This is in contrast to the behavior of the suppressed coordinate inside the axis aligned region, where it would

TABLE III. Values of the parameters (a,q) that correspond to the boundaries between alignment regions. These are obtained by three means; numerically (Num), by use of the theory of the Mathieu-type differential equations (Mathieu), and by extremizing the action functional (Action), as described in Sec. III.

	R/T			Z/T		
q	a			a		
	Num	Mathieu	Action	Num	Mathieu	Action
0.05		0.00124	0.00124		0.00126	0.00126
0.10		0.00491	0.00489		0.00517	0.00512
0.15		0.01082	0.01071		0.01210	0.01185
0.20	0.01839	0.01863	0.01829	0.02182	0.02267	0.02187
0.25		0.02791	0.02704		0.03776	0.03576
0.30	0.03708	0.03808	0.03619	0.05338	0.05850	0.05411
0.35		0.04843	0.04471		0.08626	0.07748
0.40	0.0501[a]	0.05813	0.05122	0.1071[a]	0.12267	0.10621
0.45		0.06622	0.05380		0.16960	0.14034
0.50		0.07161	0.04950	0.18[a]	0.22920	0.17964
0.60				0.3[a]	0.39600	0.27176

[a]These numerical values do not represent the boundary between axis alignment region and transition region but rather axis alignment region and two-dimensional multi-π-periodic motion. These figures are rough estimates of the boundary beyond which the system supports orbits with more than one period, depending on initial conditions.

decrease typically from 10^{-4} after the thermalization of 1000 trap periods to 10^{-9} after the thermalization of 3000 trap periods.

D. Results and discussion

In Table III, we present the results for the boundaries between alignment regions obtained from the Mathieu equation approach; from the action functional; and from direct numerical computations on the system (3).

The good agreement between direct numerical computations and the action functional approach serves as a proof of validity of the starting assumption: in the transition region π-periodic orbits can be represented as mixing between the axis aligned limit cycles of the r and z coordinates. Figure 6 shows the stability regions of the π-periodic motion within the limit cycle approximation. In the region $R(Z)$ the axis aligned motion in $r(z)$ coordinate of the system (3) is observed, i.e., the axis aligned motion described by limit cycles from Eqs. (16)–(18) and (19)–(21) is stable. The transition region T consists of the region of the MSISR where the limit cycles of both coordinates may exist and are stable [region $a(R+Z)$ in Fig. 3, but excluding the parts where the axis aligned motion may exist and is stable, regions R and Z in Fig. 6]. In the region T, transition of the alignment between r and z coordinates is observed, as well as the appearance of periodic orbits with periods that are some integer multiples of π. Though the appearance of orbits with a higher period than π was observed within the R and Z regions as well, these higher periodic orbits become dominant as the system approaches the aU region, Fig. 3.

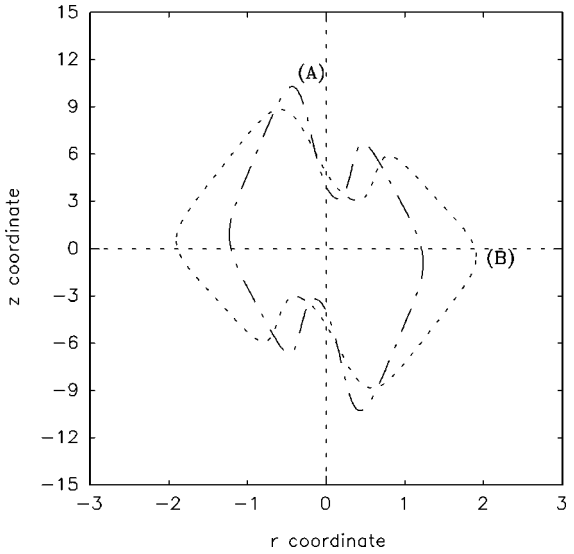

FIG. 7. Two 2π-periodic orbits are shown. (A) is obtained for $(a,q)=(0.15,\ 0.5)$ and (B) is obtained for $(a,q)=(0.2,\ 0.55)$. In both cases $\gamma=0.01$. Similarity between these two periodic orbits, obtained for two different points in the (a,q) parameter space, is demonstrated.

E. Beyond the π-periodic orbit approximation

At the outset, it is obvious that the system (3) supports, within its stability region, periodic orbits with periods that are integer multiples of the driving field period. This becomes a problem in particular when approaching the region inside the MSISR that we call the aU region, Fig. 3. Previous research has put a possible onset of chaotic behavior inside the aU region.

Our results with respect to higher period orbits are rather qualitative and rely solely on numerical computations. We can state them as follows. (i) Multiple period orbits have similar shape. In support of this we present Fig. 7. It shows the orbit with the period 2π obtained for two choices of the parameters (a,q), $(0.15,\ 0.5)$ and $(0.2,\ 0.55)$. (ii) The system (3) allows some points (a,q) in the MSISR to have more than one periodic solution depending on the initial conditions. An example is given in Fig. 8, where for the parameters $(a,q)=(0.2,\ 0.5)$ and $\gamma=0.01$ at least two stable orbits may exist. One has the period π (in this case it is a z aligned orbit), and the other has the period of 8π.

IV. DISCUSSION

The problem of ordered motion of two ions was first brought up in Ref. [7] where it was suggested, after thorough numerical simulations, that the equations of motion allow a ''crystal'' to be formed, and observed disorder was interpreted as a quasiperiodic solution of the equations of motion. As the theoretical approach for analyzing the underlying ion dynamics, a pseudopotential method was suggested [6,11]. Until now it has been the only analytical approach to the problem of a few trapped ions.

Comparison between the pseudopotential method and the limit cycle method is not simple because of the differences in the approaches and the problems they are trying to solve. The pseudopotential method concentrates on the dynamics of the secular coordinate after averaging out the micromotion.

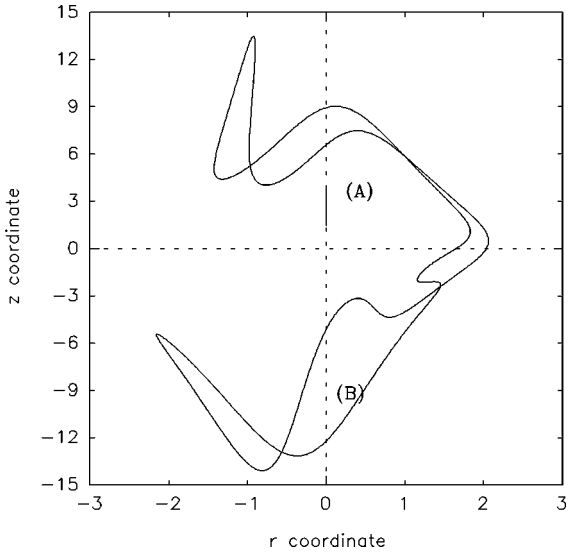

FIG. 8. Example of a periodic solution to Eq. (3), where the same point in the (a,q) parameter space yields at least two solutions with different period. (A) is a π-periodic orbit obtained for initial conditions $(r,\dot{r},z,\dot{z})_0=(5,\ 0.6,\ 8.5,\ -0.35)$ and (B) is an 8π-periodic orbit obtained for initial conditions $(r,\dot{r},z,\dot{z})_0=(10,\ 0,\ 0,\ -5)$.

The limit cycle method, on the other hand, concentrates on the micromotion and establishes how important it is for the dynamics of the ordered (π-periodic) motion. The limit cycle method gives a detailed description of the ion trajectories, their regions of stability, and the alignment of the trajectory with respect to the trap axes. Most importantly, the results predicted by the limit cycle approach are all in good agreement with the results of direct numerical computations, which is not always the case with pseudopotential results.

The limit cycles method combined with numerical simulations suggests that the disordered motion is either periodic motion with the period that is some higher integer multiple of π, or bounded aperiodic motion (chaos). This may explain the observed disordered motion found in the numerical experiments in Refs. [11,22]. Our theory suggests that disordered motion is the only possible motion if the trap parameters are inside the region aU, Fig. 3, because in that part of the parameter space no limit cycle corresponding to the ordered motion is stable.

V. CONCLUSIONS

Two ions in a Paul trap can undergo an ordered periodic motion that in mathematical terms can be described as a limit cycle with a period of the driving field of the trap. We have developed a theory of such periodic motion based on van der Pol–Krylov–Bogoliubov approximation to the limit cycle solutions of the equations of the motion and on the familiar results for Mathieu-type differential equations. We have shown that π-periodic motion may occur either as the axis aligned (along r or z axis), or off axis. The axis aligned motion can be described by a simple limit cycle, while off-axis motion can be described as mixing of the limit cycles that correspond to the axis aligned motion of each of the coordinates.

We have calculated boundaries of the alignment regions theoretically and numerically and thus found where an ordered motion (a ''crystal'') may exist. For theoretical calculations of the alignment stability boundaries we have used two approaches. In the first one we utilize the known stability regions of the solutions to Mathieu-type differential equations. We have demonstrated the existence of the transition region and calculated the boundaries between the transition region and the regions of the axis aligned motion. In the second one, we resort to an action functional approach. We have calculated (within the limit cycle approximation) the action functional in which the mixing parameter θ between the r and z coordinate limit cycles was introduced. Finding the extrema of the action functional with respect to the angle θ yields the desired behavior in the transition region and gives an independent estimate for the boundaries between the transition region and the regions for the axis aligned motion. We have found good agreement between the values obtained by these three means.

We have found that there exist periodic orbits with a period that is some integer multiple of π. We have also found that for a given point in the MSISR parameter space more than one periodic orbit is possible, depending on the initial conditions. For orbits with the same period obtained for different values of the (a,q) parameters of the trap, we have found that they are similar in shape.

We have observed that the periods of periodic orbits tend to increase when approaching the aU region, where disordered motion had been reported in Refs. [11,22]. The exact nature and the parameters that characterize these periodic orbits are beyond the scope of this paper, and are under further investigation. The nature of chaos in this system still remains to be clarified.

ACKNOWLEDGMENTS

The authors acknowledge the helpful and fruitful discussions with N. B. Jevtić, M. Mackie, and R. V. Jensen. This work was initiated while one of us (W.S.) was a guest of Professor H. Walther at the Max-Planck-Institut für Quantenoptik (Garching, Germany) with support from the Alexander von Humboldt Foundation. Later work was supported in part by Kinsley Grant No. 92K001 from the State of Connecticut Yankee Ingenuity Initiative, and by a grant from the University of Connecticut Research Foundation.

APPENDIX: EVALUATION OF CONTOUR INTEGRALS

We first evaluate the integral of the form

$$I_1=\int_0^{\pi} d\tau \frac{[C+D\ \cos(2\tau)]^2}{[A+B\ \cos(2\tau)]^3}=\frac{1}{2}\int_0^{2\pi} dy \frac{[C+D\ \cos(y)]^2}{[A+B\ \cos(y)]^3},$$

where $A>|B|>0$ and $C>|D|>0$, using the technique of contour integration. By the transformation $z=e^{iy}$, the integral becomes

$$I_1=\frac{1}{i}\oint_{\Gamma} dz \frac{[D+2Cz+Dz^2]^2}{[B+2Az+Bz^2]^3},$$

where the contour Γ is given with $|z|=1$, counterclockwise. The only pole of the denominator inside the contour Γ is

$$z_p = \frac{-A+\sqrt{A^2-B^2}}{B}.$$

Using the Cauchy theorem, we get

$$I_1 = 2\pi \operatorname*{Res}_{z\to z_p} \frac{[D+2Cz+Dz^2]^2}{[B+2Az+Bz^2]^3}$$

$$= \frac{\pi}{2} \frac{2A^2C^2+B^2C^2-6ABCD+A^2D^2+2B^2D^2}{(A^2-B^2)^{5/2}}.$$

In the computations A,B,C,D are replaced with the values appropriate for the limit cycles. We recall that the limit cycle of the r coordinate is given by $r_{\rm lim}=r_0+\delta r\ \cos(2\tau)$ with $r_0,\delta r>0$ and $z_{\rm lim}=z_0-\delta z\ \cos(2\tau)$ with $z_0,\delta z>0$.

Under these circumstances, the second integral is even simpler. We have

$$I_2 = \int_0^{\pi} d\tau \frac{1}{A+B\ \cos(2\tau)} = \frac{1}{2}\int_0^{2\pi} dy \frac{1}{A+B\ \cos(y)}.$$

Using the same substitution $z=e^{iy}$, it becomes a contour integral along the same contour Γ as the integral I_1,

$$I_2 = \frac{1}{i}\oint_{\Gamma} dz \frac{1}{B+2Az+Bz^2}.$$

Contour integration then gives

$$I_2 = 2\pi \operatorname*{Res}_{z\to z_p} \frac{1}{B+2Az+Bz^2} = \frac{\pi}{\sqrt{A^2-B^2}}.$$

[1] W. Paul, Rev. Mod. Phys. **62**, 531 (1990).
[2] R. Blatt, P. Gill, and R. C. Thompson, J. Mod. Opt. **39**, 193 (1992).
[3] R. F. Wuerker, H. Shelton, and R. V. Langmuir, J. Appl. Phys. **30**, 342 (1959).
[4] F. Diedrich, E. Peik, J. M. Chen, W. Quint, and H. Walther, Phys. Rev. Lett. **59**, 2931 (1987).
[5] D. J. Wineland, J. C. Bergquist, W. M. Itano, J. J. Bollinger, and C. H. Manney, Phys. Rev. Lett. **59**, 2935 (1987).
[6] J. Hoffnagle, R. G. DeVoe, L. Reyna, and R. G. Brewer, Phys. Rev. Lett. **61**, 255 (1988).
[7] R. Blümel *et al.*, Phys. Rev. A **40**, 808 (1989).
[8] S. A. Prasad and T. M. O'Neil, Phys. Fluids **22**, 278 (1979).
[9] L. D. Landau, E. M. Lifschitz, and A. I. Akhezier, *General Physics; Mechanics and Molecular Physics* (Pergamon Press, Oxford, 1967).
[10] J. W. Emmert *et al.*, Phys. Rev. A **48**, R1757 (1993).
[11] M. G. Moore and R. Blümel, Phys. Rev. A **50**, R4453 (1994).
[12] M. Humi and W. Miller, *Second Course in Ordinary Differential Equations for Scientists and Engineers* (Springer-Verlag, New York, 1988), Chap. 7.
[13] S. Lefschetz, *Differential Equations: Geometric Theory* (Dover, New York, 1977), pp. 312–345.
[14] R. Blümel, Phys. Rev. A **51**, 620 (1995).
[15] W. D. Lakin and D. A. Sanchez, *Topics in Ordinary Differential Equations* (Dover, New York, 1982), pp. 109–111.
[16] P. W. Jordan and P. Smith, *Nonlinear Ordinary Differential Equations* (Clarendon Press, Oxford, 1977), pp. 237–245.
[17] A. H. Naypeh and D. T. Mook, *Nonlinear Oscillations* (Wiley, New York, 1979), pp. 270–283.
[18] L. Ott, *An Introduction to Statistical Methods and Data Analysis* (PWS Kent Publishing Company, Boston, 1988).
[19] Y. Yan-Qian, *Theory of Limit Cycles, Translations of Mathematical Monographs* (American Mathematical Society, Providence, 1965), Vol. 66, Chaps. 1–3.
[20] J. G. Papastavridis, J. Sound Vib. **74**, 499 (1981).
[21] D. Y. Hsieh, J. Math. Phys. **19**, 1147 (1978).
[22] M. A. Mackie, R. V. Jensen, and W. W. Smith (unpublished).